



HHS Public Access

Author manuscript

J Mater Chem C Mater Opt Electron Devices. Author manuscript; available in PMC 2017 November 28.

Published in final edited form as:

J Mater Chem C Mater Opt Electron Devices. 2016 November 28; 4(44): 10554–10561. doi:10.1039/C6TC03666J.

Photoexcited State Properties of Carbon Dots from Thermally Induced Functionalization of Carbon Nanoparticles

Yin Hu[†], Mohamad M. Al Awak[‡], Fan Yang[†], Sijia Yan[†], Qingwu Xiong[†], Ping Wang[†], Yongan Tang[¶], Liju Yang^{‡,*}, Gregory E. LeCroy[†], Xiaofang Hou[†], Christopher E. Bunker[§], Linxi Xu[†], Nicholas Tomlinson[†], and Ya-Ping Sun^{†,*}

[†]Department of Chemistry and Laboratory for Emerging Materials and Technology, Clemson University, Clemson, South Carolina 29634, USA

[‡]Department of Pharmaceutical Sciences, Biomanufacturing Research Institute and Technology Enterprise, North Carolina Central University, Durham, NC 27707, USA

[¶]Department of Mathematics and Physics, North Carolina Central University, Durham, NC 27707, USA

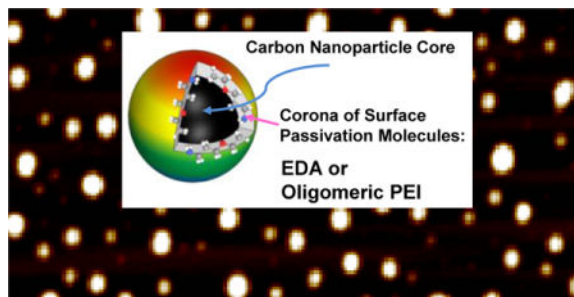
[§]Air Force Research Laboratory, Propulsion Directorate, Wright-Patterson Air Force Base, Ohio 45433, USA

Abstract

Carbon dots are small carbon nanoparticles with various surface passivation schemes, in which more effective has been the deliberate chemical functionalization of the nanoparticles for brighter fluorescence emissions, though the synthesis method is more tedious and subject to some limitations in the selection of functionalization molecules. Another more popular synthesis method has been the carbonization of organic species, with the method being more efficient and versatile, but less controllable in the synthesis and for the desired dot structure and performance. In this work, a hybrid approach combining the advantageous characteristics of the two synthesis methods was applied to the preparation of carbon dots with polyethyleneimine (PEI) for surface passivation, where pre-processed and selected small carbon nanoparticles were functionalized with PEI in microwave-induced thermal reactions. The optical absorption and fluorescence emission properties were evaluated, and the results suggested that the carbon dots thus prepared shared the same photoexcited state characteristics with those from the deliberate chemical functionalization, including comparable fluorescence colors and other properties. A further demonstration on the similarity in photoexcited state properties was based on the same visible light-activated bactericidal functions of the PEI-carbon dots as those found in carbon dots from the deliberate chemical functionalization. The advantages and potential limitations of the hybrid approach for more controllable yet versatile and efficient syntheses of carbon dots are highlighted and discussed.

Graphical abstract

*Corresponding Authors: lyang@ncu.edu, syaping@clemson.edu.



Carbon dots prepared by using a hybrid approach are demonstrated for photoexcited state properties and bactericidal activities.

Introduction

Carbon “quantum” dots or more appropriately named as carbon dots (for the lack of the classical quantum confinement in these fluorescent carbon nanomaterials)^{1–3} have attracted much recent attention,^{2–9} from simple curiosity or fascination on the fact that any “carbon dirt” could be made to exhibit colorful fluorescence emissions,^{8–15} to the exploration of their various potential technological applications.^{2–4,8,16–20} In fact, with a quick search of the recent literature one would conclude that carbon dots research has emerged as a highly active and rapidly expanding field, whose broad impacts similar to or even beyond those already derived from conventional semiconductor quantum dots (QDs)^{21–26} may be envisaged.

Carbon dots are generally small carbon nanoparticles with various surface passivation schemes (Figure 1),^{1–3} in which more effective has been surface functionalization of the nanoparticles by organic molecules or biological species for more intense fluorescence emissions in the visible spectrum, extending into the near-IR.^{2–4,27} Among the more popular approaches in the synthesis of carbon dots have been the deliberate chemical functionalization of small carbon nanoparticles^{1,27–29} and the carbonization (often in “one-pot”) of organic or other carbon-containing precursors.^{2,8,30,31} The deliberate functionalization approach has been successful in terms of producing structurally well-defined carbon dots of high fluorescence quantum yields (more than 50% in some configurations),²⁷ but the synthesis is more tedious and subject to some limitations in the selection of molecules for functionalization. The carbonization approach is more efficient and versatile, compatible with a diverse selection of precursors and functionalization molecules or species, but less controllable both in the synthesis and for the desired structures of produced carbon dots, among other processing and performance issues.^{2–4,6,8} Thus, an interesting and useful strategy is to combine the advantageous characteristics of the two synthetic approaches for more controllable yet efficient and versatile preparations of carbon dots. Specifically for such a hybrid approach,³² the pre-processed and selected small carbon nanoparticles are used as precursor, but instead of chemical functionalization reactions, the molecules or species designed for surface passivation are “attached to” (or more like “welded onto”) the carbon nanoparticles in thermally induced reactions, in which the molecules for passivation may also be slightly or partially carbonized in the reactions

(Figure 1). Nevertheless, the hybrid approach still adheres closely to the definition of carbon dots as surface-passivated small carbon nanoparticles.

In this work, the hybrid approach was applied to the preparation of carbon dots with polyethyleneimine (PEI) for surface passivation (Figure 1), where small carbon nanoparticles from the processing of a commercially supplied carbon nanopowder sample were functionalized with PEI in microwave-induced thermal reactions. The optical absorption and fluorescence emission properties were evaluated, and the results suggested that the carbon dots thus prepared shared the same photoexcited state characteristics with those synthesized by the deliberate chemical functionalization approach (such as the carbon dots with EDA for surface functionalization, Figure 1), including comparable fluorescence colors and other properties. A further demonstration on the similarity in photoexcited state properties was based on the same visible light-activated bactericidal functions of the PEI-carbon dots as those found in carbon dots synthesized by the deliberate chemical functionalization approach. The advantages and potential limitations of the hybrid approach for more controllable yet versatile and efficient syntheses of carbon dots with desired photoexcited state properties are highlighted and discussed.

Results and Discussion

A commercially acquired carbon nanopowder sample was used as precursor in the processing to harvest small carbon nanoparticles. Briefly, the as-supplied carbon nanopowder sample was refluxed in nitric acid, followed by dialysis and centrifugation to obtain mostly smaller carbon nanoparticles in an aqueous suspension,²⁹ which appeared transparent and solution-like. The observed absorption spectrum of the suspension was similar to those of similarly processed carbon nanoparticles reported previously, so were the relatively weak fluorescence emission spectra.^{33–35} According to atomic force microscopy (AFM) results, these particles were on the order of 5 nm in diameter, also similar to those reported previously.

For the functionalization of the carbon nanoparticles was an oligomeric polyethyleneimine (PEI) of a more branched structure, with a significant number of primary amine moieties and structurally more compact. Experimentally, the carbon nanoparticles were mixed with PEI and a small amount of ethanol via vigorous sonication at a temperature slightly above the ambient, followed by the removal of ethanol via evaporation. The resulting mixture was heated in a conventional microwave oven by following a multiple-cycle regiment such that the sample was heated until smoke started to appear, cooled in the ambient for a short period of time, and repeats of the same heating and cooling processes for a total of up to 30 heating-cooling cycles. Post-processing, the sample back at ambient temperature was dispersed in water with vigorous sonication. The resulting aqueous dispersion was centrifuged at 20,000 *g* to collect the supernatant, followed by dialysis in a membrane tubing against fresh water to remove unreacted PEI and other small molecular impurities to obtain the PEI-carbon dots as a clear colored solution (Figure 2). Results from AFM analyses of the PEI-carbon dots sample suggest that these dots are size-wise relatively narrowly distributed, on average 6.5 nm in diameter with the size distribution standard deviation of a little more than 1 nm (Figure 3).

The absorption spectrum of the PEI-carbon dots in aqueous solution is shown in Figure 2, which is similar to those of the precursor carbon nanoparticles and also carbon dots prepared from deliberate chemical functionalization (such as the EDA-carbon dots, Figure 2),²⁹ supporting the notion that the optical absorption in carbon dots is due to electronic transitions in the core carbon nanoparticles.³⁶ Also shown in Figure 2 is the fluorescence spectrum of the PEI-carbon dots in aqueous solution at 400 nm excitation, which is again comparable with that of the EDA-carbon dots.²⁹

The PEI-carbon dots in solution were characterized by using solution-phase NMR technique, and the results were compared with those of free PEI used in the functionalization reaction. As shown in Figure 4, the proton NMR signals of the PEI-carbon dots in deuterated water are significantly broader than those of free PEI, consistent with the expected lower mobility of the PEI species attached to carbon nanoparticles.³⁷ Similar broadening effect was observed in carbon dots prepared by deliberate chemical functionalization with small organic molecules, such as in the EDA-carbon dots,²⁹ though to a somewhat lesser extent, because signals of the free PEI are already broad (Figure 4). Overall, the proton NMR signals of the PEI-carbon dots in reference to those of free PEI could be assigned to two groups, one for the α protons, downfield-shifted from that of free PEI (Figure 4), which might be attributed to some de-shielding effect resulted from the binding and/or strong interactions of the amino groups with carbon nanoparticles; and the other for the β and γ protons (Figure 4). The relative integrations between the α and $\beta+\gamma$ proton signals (1-to-1.1) are unchanged from free PEI to the PEI-carbon dots, suggesting no major structural changes in the particle-bound PEI species.

Fluorescence spectra of the PEI-carbon dots in aqueous solution were also measured more systematically as a function of excitation wavelengths. Similar to those found in carbon dots from other syntheses (again the EDA-carbon dots, for example),²⁹ the excitation wavelength dependence exhibited progressive red shifts and a narrowing of the emission band width with excitation at longer wavelengths (Figure 5). The excitation wavelength dependence of fluorescence quantum yields followed a similar pattern, as also shown in Figure 5, again similar to those of carbon dots obtained from other syntheses.^{1,29,35} The dependencies of fluorescence spectra and quantum yields on excitation wavelengths have been rationalized previously as being associated with the selective access of different collections of emissive excited states, with less states accessed at longer wavelength excitations.^{1,36}

Fluorescence decays of the PEI-carbon dots were measured by using the time-correlated single photon counting (TCSPC) technique (Figure 6). The observed decays at both 400 nm and 440 nm excitations could be deconvoluted with a bi-exponential function, and the results are shown in Table 1. It should be pointed out that despite the good deconvolution fits, the excited states and processes in the carbon dots are likely more complicated than only two emission contributions. Nevertheless, the phenomenological bi-exponential fits provide a reasonable averaging for the likely multi-component decay processes in these carbon dots. For the purpose of a more direct comparison, a further averaging was made by using the pre-exponential factors (A_1 and A_2) and lifetimes (τ_{F1} and τ_{F2}) from the deconvolution fits, $\langle \tau_F \rangle = (A_1 \tau_{F1}^2 + A_2 \tau_{F2}^2) / (A_1 \tau_{F1} + A_2 \tau_{F2})$,³⁸ and the average fluorescence lifetime $\langle \tau \rangle$ values thus calculated are also shown in Table 1. These lifetime results are roughly

comparable with those of the carbon dots from deliberate chemical functionalization syntheses.^{27,35}

The spectroscopic results presented above suggest that the PEI-carbon dots obtained from thermally induced functionalization of small carbon nanoparticles by the PEI molecules are similar to carbon dots from more controlled chemical functionalization syntheses in terms of their optical transitions and fluorescence emissions, which reflect upon their associated excited state properties. From a somewhat different angle, the photoexcited state properties of carbon dots have been investigated by examining their photodynamic effects,⁴ including for example the use of carbon dots for photoinduced killing of cancer cells^{39–41} and also more recently for the visible light-driven bactericidal functions of the EDA-carbon dots.⁴² Thus, the PEI-carbon dots obtained from the thermally induced functionalization were also evaluated for their ability with visible light activation to inhibit bacterial growth.

Bacillus subtilis, a Gram-positive bacterium, has been a popular laboratory model organism and often considered as the Gram-positive equivalent of *Escherichia coli*, an extensively studied Gram-negative bacterium.^{43–45} It was used in the evaluation on the visible light-activated antibacterial function of the PEI-carbon dots. Experimentally, a suspension of the cultured bacterial cells and an aqueous solution of the PEI-carbon dots were added to multiple-well plates, with the final bacterial cell concentration in each well of about 10⁶ CFU/mL and the concentration of the PEI-carbon dots varied as needed (triplicates for each concentration). The plates were either exposed to visible light or kept in the dark for a pre-determined period of time. Immediately after treatment, the treated samples and the controls were serially diluted for the determination of the viable cell numbers by using the traditional plating method. The reduction in viable cell number in the samples treated with the PEI-carbon dots and light in comparison to the controls was used as a measure for the efficiency of the light-activated bactericidal function. As shown in Figure 7, for the sample treated with 0.02 mg/mL PEI-carbon dots, there were ~2.5 log viable cell reductions with 1 h light illumination, versus about 0.5 log reductions in the dark controls, indicating the substantial effect of visible light activation. The results are generally consistent with those from similar studies in which carbon dots from other syntheses were used.⁴² However, the apparently somewhat significant antibacterial effect of the PEI-carbon dots even in the absence of light activation is puzzling. In addition to experimental factors such as the high sensitivity of the bactericidal function of carbon dots to even minimal ambient light exposure,⁴² the carbon nanoparticle-bound PEI species might have some surfactant-like properties, slightly inhibitive to the bacterial cell growth in the dark controls. Nevertheless, the visible light activation obviously made the PEI-carbon dots orders of magnitude more effective in the inhibition of *B. subtilis*. The bacteria inhibition may be attributed to photodynamic effect,⁴² similar to what has been reported on the use of conventional semiconductor nanomaterials.^{46–49}

Similar to carbon dots from other syntheses,^{27,29} the sample of PEI-carbon dots from the thermally induced functionalization in this work contained a mixture of various fractions with different fluorescence performances. The more fluorescent fractions could be harvested via separation on an aqueous gel column, as similarly practiced and reported previously.^{27,29} The aqueous gel column was packed in house by using commercially acquired Sephadex™

G-100 gel. In the fractionation, the sample of PEI-carbon dots was added to the column and eluted with water, and colored fractions were collected and characterized. The more fluorescent fractions (fluorescence quantum yields around 20% at 400 nm excitation) were combined into one sample, as the observed absorption and fluorescence spectra among the fractions were rather similar. For the more fluorescent sample thus obtained, its absorption and fluorescence spectra are similar to those of the as-synthesized sample pre-fractionation (Figure 2). Interestingly, however, despite the significantly higher fluorescence quantum yields (Table 1), the more fluorescent sample from the fractionation exhibited fluorescence decays similar to those of the as-synthesized sample pre-fractionation (Figure 6, Table 1). Such a decoupling between changes in fluorescence quantum yields and decays (or average fluorescence lifetimes, Table 1) reflects upon the likely more complicated photoexcited state properties and processes in carbon dots, with significant mechanistic implications.

Mechanistically, the fluorescence emissions in carbon dots are attributed to radiative recombinations of photo-generated electrons and holes trapped at diverse surface defect sites.^{17,35,50} Experimental evidence for the involvement of electrons and holes included the results on highly efficient fluorescence quenching of carbon dots by both electron donors and acceptors,⁵⁰ and the harvesting of the photo-generated electrons for various reactions such as the reduction of carbon dioxide into small organic molecules.^{2,17,51} Within such a mechanistic framework, the apparent decoupling between the observed fluorescence quantum yields and decays may be rationalized by the presence of two primary excited state processes following the initial photoexcitation, one for the formation (or populating) of the emissive excited states and the other for the deactivation of these states via fluorescence emissions and competing nonradiative pathways.³⁸ Thus, with quantum yields for the former denoted as Φ_1 and for the radiative process in the latter as Φ_2 , the observed fluorescence quantum yields (Φ_F) must be reflecting a combination of the two processes, $\Phi_F = \Phi_1\Phi_2$. The first process represented by Φ_1 was apparently too fast to be captured in the fluorescence decay measurements, where the time resolution in terms of the instrument response function was on the order of 100–200 ps, so that the observed fluorescence decays were associated only with the deactivation process of the emissive excited states. Thus, the average fluorescence lifetimes (Table 1) are coupled with the quantum yields Φ_2 for the radiative pathway in the second process. In general, carbon dots with more effective surface passivation have exhibited brighter fluorescence emissions and correspondingly higher fluorescence quantum yields.^{3,27,35} As such, the more fluorescent sample from the gel column fractionation was likely composed of carbon dots with more effective passivation by the surface-bound PEI species. Based on the discussion above, such enhanced fluorescence emissions and quantum yields must be due primarily to larger Φ_1 values. However, mechanistic details on how the improved surface passivation in carbon dots makes the Φ_1 process more efficient are yet to be probed and understood.

Conclusions

Thermally induced functionalization of pre-processed and selected small carbon nanoparticles with the oligomeric PEI yielded carbon dots of optical absorption and fluorescence properties similar to those of the dots synthesized by the deliberate chemical functionalization method. The similarity in photoexcited state properties is also reflected in

the observed visible light-activated bactericidal functions of the PEI-carbon dots. The results provide a clear validation on the hybrid approach for the preparation of carbon dots that combines the advantageous characteristics in the method of deliberate chemical functionalization synthesis and the method based on the carbonization of organic and other carbon-containing precursors. Carbon dots prepared by the deliberate chemical functionalization method are generally nontoxic according to available results from cytotoxicity and *in vivo* toxicity studies.^{3,4,16,52–54} Similar investigations on the PEI-carbon dots will be pursued.

Experimental Section

Materials

The carbon nanopowder sample was purchased from US Research Nanomaterials, Inc., polyethyleneimine (PEI, branched, average molecular weight ~1,200) from Polyscience, Inc., and silicon carbide (120 Grit) from Panadyne Abrasives. Nitric acid was obtained from Fisher Scientific, and deuterated water for NMR experiments from Cambridge Isotope Laboratories. The dialysis membrane tubings (molecular weight cut-off ~500 and ~1,000) were supplied by Spectrum Laboratories. Water was deionized and purified by passing through a Labconco WaterPros water purification system.

Measurement

UV/vis absorption spectra were recorded on a Shimadzu UV2501-PC spectrophotometer. Fluorescence spectra were acquired on a Jobin-Yvon emission spectrometer equipped with a 450 W xenon source, Gemini-180 excitation and Tirax-550 emission monochromators, and a photon counting detector (Hamamatsu R928P PMT at 950 V). 9,10-Bis(phenylethynyl)-anthracene in cyclohexane was used as a standard in the determination of fluorescence quantum yields by the relative method (matching the absorbance at the excitation wavelength between the sample and standard solutions and comparing their corresponding integrated total fluorescence intensities). Fluorescence decays were measured in terms of the time-correlated single photon counting (TCSPC) technique on a Horiba Ultima Extreme spectrometer. The spectrometer is equipped with a SuperK Extreme supercontinuum laser source operated at 3.894 MHz repetition rate, TDM-800 excitation and TDM-1200 emission monochromators, a R3809-50 MCP-PMT detector operated at 3.0 KV in a thermoelectrically cooled housing, and FluoroHub A+ timing electronics. Analyses of the decay curves were performed by using the Horiba Das6 fluorescence decay analysis software. NMR measurements were carried out on a Bruker Advance 500 NMR spectrometer. Atomic force microscopy (AFM) images were acquired in the acoustic AC mode on a Molecular Imaging PicoPlus AFM system equipped with a multipurpose scanner and a NanoWorld point probe NCH sensor. The height profile analysis was assisted by using the SjPIP software distributed by Image Metrology.

Carbon Dots

Small carbon nanoparticles were harvested from the commercially acquired carbon nanopowder sample in a procedure similar to those reported previously.^{29,35} In a typical experiment, the carbon nanopowder sample (2 g) was refluxed in aqueous nitric acid (8 M,

200 mL) for 48 h. The reaction mixture was cooled to room temperature, and centrifuged at 1,000 *g* to discard the supernatant. The residue was re-dispersed in deionized water, dialyzed in a membrane tubing (molecular weight cut-off ~500) against fresh water for 48 h, and then centrifuged at 1,000 *g* to retain the supernatant. Upon the removal of water, carbon nanoparticles were recovered.

Carbon nanoparticles obtained from the processing above (100 mg) were mixed with PEI (2 g) and ethanol (1 mL) in a scintillation vial, and the mixture was sonicated (ultrasonic cleaner, VWR 250D) at 40 °C for 1 h, followed by the removal of ethanol via evaporation. Separately, a silicon carbide bath was prepared by placing silicon carbide (170 g) in a silica crucible casting dish (about 8 cm in diameter and 2.5 cm in height). The bath was pre-heated in a conventional microwave oven at 500 W for 3 min, and then the vial containing the mixture of carbon nanoparticles and PEI was immersed in the bath, followed by the microwave treatment in multiple cycles. In each cycle, the mixture in the bath was irradiated at 400 W until smoke started to appear. Upon the irradiation for another 30 s, the vial containing the mixture was taken out of the bath for 1 min in the ambient, and then immersed in the bath again for the next treatment cycle. After the microwave treatment of up to 30 heating-cooling cycles, the reaction mixture was cooled to the ambient temperature and dispersed in deionized water (10 mL) with vigorous sonication. The resulting aqueous dispersion was centrifuged at 20,000 *g* for 30 min to collect the supernatant, followed by dialysis against fresh water for 24 h. The as-synthesized sample of the PEI-carbon dots was obtained as a colored aqueous solution. ¹H NMR (500 MHz, D₂O) δ 2.71 (m, br), 2.60 (m, br), 2.42 (m, br), 2.38 (m, br) ppm.

For more fluorescent PEI-carbon dots, the as-synthesized sample was separated on an aqueous gel column. The column was packed with the commercially supplied Sephadex™ G-100 gel by following the previously reported protocol.²⁷ Briefly, the gel (15 g) was soaked in water for 3 days, and the supernatant (including the suspended ultrafine gel) was discarded. The remaining gel was washed until no gel was suspended in the supernatant. Air bubbles were removed under vacuum. Separately, a glass column (25 mm inner diameter) was filled with water to remove air bubbles, and then closed. The gel suspension described above was poured into the column until reaching about 2 cm in height, and then the column was opened for the continuous addition of the gel suspension. The gel column was washed with water until no change in the height, followed by the testing and calibration.²⁷ In the fractionation of the as-synthesized PEI-carbon dots sample, a concentrated solution of the sample was added to the gel column and eluted with water. Colored fractions (80 drops per fraction) were collected for characterization and further investigations.

Light-Activated Bactericidal Functions

Fresh grown *B. subtilis* cells in nutrient broth (Fisher Scientific, Pittsburgh, PA) were washed three times with PBS and then re-suspended in PBS. With the use of 96-well plates, to each well was added 150 μL bacteria cell suspension and 50 μL the PEI-carbon dots solution. The final bacterial cell concentration in each well was about 10⁶ CFU/mL and the concentration of the carbon dots was varied as needed (triplicates for each concentration). The plates were either exposed to visible light (12 V 36 W light bulb) or kept in dark for 1 h.

Immediately after the treatments, the samples were serially diluted in PBS. The viable cell numbers in the control and treated samples were determined by the traditional plating method. For each sample, aliquots of 100 μL appropriate dilutions were surface-plated on Luria-Bertani agar plates (Fisher Scientific, Pittsburgh, PA). After 24 h incubation at 37 $^{\circ}\text{C}$, the number of colonies was counted and the viable cell number was calculated in colony forming units per milliliter (CFU/mL) for all treated samples and the control. The reduction in viable cell number in the carbon dots-treated samples in comparison to the control was used to evaluate the efficiency of bactericidal function of the PEI-carbon dots.

Acknowledgments

Financial support from NIH (R15GM114752) and the Air Force Office of Scientific Research through the program of Dr. Charles Lee (Y.-P.S.) is gratefully acknowledged. Y.H. was a visiting student from Beijing Jiaotong University (China) and S.Y. and Q.X. were visiting students from Shantou University (China), with the visits sponsored by the China Scholarship Council and NSFC (51272152 and 21671127), respectively, and L.X. and N.T. were participants of the Palmetto Academy funded and managed by the South Carolina Space Grant Consortium.

References

1. Sun YP, Zhou B, Lin Y, Wang W, Fernando KAS, Pathak P, Meziani MJ, Harruff BA, Wang X, Wang HF, Luo PG, Yang H, Kose ME, Chen BL, Veca LM, Xie SY. *J Am Chem Soc.* 2006; 128:7756–7757. [PubMed: 16771487]
2. Fernando KAS, Sahu S, Liu Y, Lewis WK, Gulians EA, Jafariyan A, Wang P, Bunker CE, Sun YP. *ACS Appl Mater Interfaces.* 2015; 7:8363–8376. [PubMed: 25845394]
3. LeCroy GE, Yang ST, Yang F, Liu Y, Fernando KAS, Bunker CE, Hu Y, Luo PG, Sun YP. *Coord Chem Rev.* 2016; 320:66–81.
4. Luo PG, Yang F, Yang ST, Sonkar SK, Yang L, Broglie JJ, Liu Y, Sun YP. *RSC Adv.* 2014; 4:10791–10807.
5. Hola K, Zhang Y, Wang Y, Giannelis EP, Zboril R, Rogach AL. *Nano Today.* 2014; 9:590–603.
6. Wang Y, Hu A. *J Mater Chem C.* 2014; 2:6921–6939.
7. Miao P, Han K, Tang Y, Wang B, Lin T, Cheng W. *Nanoscale.* 2015; 7:1586–1595. [PubMed: 25510876]
8. Lim SY, Shen W, Gao Z. *Chem Soc Rev.* 2015; 44:362–381. [PubMed: 25316556]
9. Du Y, Guo S. *Nanoscale.* 2016; 8:2532–2543. [PubMed: 26757977]
10. Liu SS, Wang CF, Li CX, Wang J, Mao LH, Chen S. *J Mater Chem C.* 2014; 2:6477–6483.
11. Lin PY, Hsieh CW, Kung ML, Chu LY, Huang HJ, Chen HT, Wu DC, Kuo CH, Hsieh SL, Hsieh S. *J Biotechnol.* 2014; 189:114–119. [PubMed: 25225122]
12. Liu R, Zhang J, Gao M, Li Z, Chen J, Wu D, Liu P. *RSC Adv.* 2015; 5:4428–4433.
13. Xu J, Lai T, Feng Z, Weng X, Huang C. *Luminescence.* 2015; 30:420–424. [PubMed: 25158918]
14. D'Angelis do ES B, Corrêa JR, Medeiros GA, Barreto G, Magalhães KG, de Oliveira AL, Spencer J, Rodrigues MO, Neto BA. *Chem Eur J.* 2015; 21:5055–5060. [PubMed: 25693878]
15. Essner JB, Laber CH, Ravula S, Polo-Parada L, Baker GA. *Green Chem.* 2016; 18:243–250.
16. Yang ST, Cao L, Luo PG, Lu F, Wang X, Wang H, Meziani MJ, Liu Y, Qi G, Sun YP. *J Am Chem Soc.* 2009; 131:11308–11309. [PubMed: 19722643]
17. Cao L, Sahu S, Anilkumar P, Bunker CE, Xu J, Fernando KAS, Wang P, Gulians EA, Tackett KN, Sun YP. *J Am Chem Soc.* 2011; 133:4754–4757. [PubMed: 21401091]
18. Dong Y, Wang R, Li G, Chen C, Chi Y, Chen G. *Anal Chem.* 2012; 84:6220–6224. [PubMed: 22686413]
19. Zhu S, Meng Q, Wang L, Zhang J, Song Y, Jin H, Zhang K, Sun H, Wang H, Yang B. *Angew Chem Int Ed.* 2013; 52:3953–3957.
20. Zhao A, Chen Z, Zhao C, Gao N, Ren J, Qu X. *Carbon.* 2015; 85:309–327.

21. Holmes JD, Ziegler KJ, Doty RC, Pell LE, Johnston KP, Korgel BA. *J Am Chem Soc.* 2001; 123:3743–3748. [PubMed: 11457106]
22. Li Z, Ruckenstein E. *Nano Lett.* 2004; 4:1463–1467.
23. Lambert TN, Andrews NL, Gerung H, Boyle TJ, Oliver JM, Wilson BS, Han SM. *Small.* 2007; 3:691–699. [PubMed: 17299826]
24. Erogbogbo F, Yong KT, Roy I, Xu G, Prasad PN, Swihart MT. *ACS Nano.* 2008; 2:873–878. [PubMed: 19206483]
25. Prabakar S, Shiohara A, Hanada S, Fujioka K, Yamamoto K, Tilley RD. *Chem Mater.* 2009; 22:482–486.
26. Kang Z, Liu Y, Lee ST. *Nanoscale.* 2011; 3:777–791. [PubMed: 21161100]
27. Wang X, Cao L, Yang ST, Lu F, Mezziani MJ, Tian L, Sun KW, Bloodgood MA, Sun YP. *Angew Chem Int Ed.* 2010; 122:5438–5442.
28. Anilkumar P, Wang X, Cao L, Sahu S, Liu J-H, Wang P, Korch K, Tackett KN II, Parenzan A, Sun Y-P. *Nanoscale.* 2011; 3:2023–2027. [PubMed: 21350751]
29. LeCroy GE, Sonkar SK, Yang F, Veca LM, Wang P, Tackett KN II, Yu J-J, Vasile E, Qian H, Liu Y, Luo PG, Sun Y-P. *ACS Nano.* 2014; 8:4522–4529. [PubMed: 24702526]
30. Hsu PC, Chang HT. *Chem Commun.* 2012; 48:3984–3986.
31. Stan C, Albu C, Coroaba A, Popa M, Sutiman D. *J Mater Chem C.* 2015; 3:789–795.
32. Rednic MI, Lu Z, Wang P, LeCroy GE, Yang F, Liu Y, Qian H, Terec A, Veca LM, Lu F, Sun YP. *Chem Phys Lett.* 2015; 639:109–113.
33. Ray SC, Saha A, Jana NR, Sarkar R. *J Phys Chem C.* 2009; 113:18546–18551.
34. Cao L, Anilkumar P, Wang X, Liu JH, Sahu S, Mezziani MJ, Myers E, Sun YP. *Can J Chem.* 2010; 89:104–109.
35. Liu Y, Wang P, Fernando KAS, LeCroy GE, Maimaiti H, Harruff-Miller BA, Lewis WK, Bunker CE, Hou ZL, Sun YP. *J Mater Chem C.* 2016; 4:6967–6974.
36. Cao L, Mezziani MJ, Sahu S, Sun YP. *Acc Chem Res.* 2013; 46:171–180. [PubMed: 23092181]
37. Terrill RH, Postlethwaite TA, Chen C-h, Poon C-D, Terzis A, Chen A, Hutchison JE, Clark MR, Wignall G. *J Am Chem Soc.* 1995; 117:12537–12548.
38. Lakowicz, RJ. *Principles of fluorescence spectroscopy.* 2nd. Kluwer Academic/Plenum Publisher; New York: 1999.
39. Kleinauskas A, Rocha S, Sahu S, Sun YP, Juzenas P. *Nanotechnology.* 2013; 24:325103. [PubMed: 23868054]
40. Choi Y, Kim S, Choi MH, Ryoo SR, Park J, Min DH, Kim BS. *Adv Funct Mater.* 2014; 24:5781–5789.
41. Wang H, Cao G, Gai Z, Hong K, Banerjee P, Zhou S. *Nanoscale.* 2015; 7:7885–7895. [PubMed: 25854197]
42. Mezziani MJ, Dong X, Zhu L, Jones LP, LeCroy GE, Yang F, Wang S, Wang P, Zhao Y, Yang L, Tripp RA, Sun YP. *ACS Appl Mater Interfaces.* 2016; 8:10761–10766. [PubMed: 27064729]
43. Graumann, P. *Bacillus: Cellular and Molecular Biology.* 2nd. Horizon Scientific Press; Germany: 2012.
44. Govind P. *Int Res J Pharm.* 2011; 2911:62–65.
45. Mukherjee S, Kearns DB. *Annu Rev Genet.* 2014; 48:319–340. [PubMed: 25251856]
46. Matsunaga T, Tomoda R, Nakajima T, Nakamura N, Komine T. *Appl Environ Microbiol.* 1988; 54:1330–1333. [PubMed: 3046487]
47. Sunada K, Watanabe T, Hashimoto K. *J Photochem Photobiol A.* 2003; 156:227–233.
48. Cho M, Chung H, Choi W, Yoon J. *Appl Environ Microbiol.* 2005; 71:270–275. [PubMed: 15640197]
49. Garcez AS, Núñez SC, Baptista MS, Daghestanli NA, Itri R, Hamblin MR, Ribeiro MS. *Photochem Photobiol Sci.* 2011; 10:483–490. [PubMed: 21125123]
50. Wang X, Cao L, Lu F, Mezziani MJ, Li H, Qi G, Zhou B, Harruff BA, Kermarrec F, Sun YP. *Chem Commun.* 2009:3774–3776.

51. Sahu S, Liu Y, Wang P, Bunker CE, Fernando KAS, Lewis WK, Gulians EA, Yang F, Wang J, Sun YP. *Langmuir*. 2014; 30:8631–8636. [PubMed: 24972094]
52. Yang ST, Wang X, Wang H, Lu F, Luo PG, Cao L, Meziani MJ, Liu JH, Liu Y, Chen M, Huang Y, Sun YP. *J Phys Chem C*. 2009; 113:18110–18114.
53. Wang Y, Anilkumar P, Cao L, Liu JH, Luo PG, Tackett KN, Sahu S, Wang P, Wang X, Sun YP. *Exp Bio Med*. 2011; 236:1231–1238.
54. Liu JH, Cao L, LeCroy GE, Wang P, Meziani MJ, Dong Y, Liu Y, Luo PG, Sun YP. *ACS Appl Mater Interfaces*. 2015; 7:19439–19445. [PubMed: 26262834]

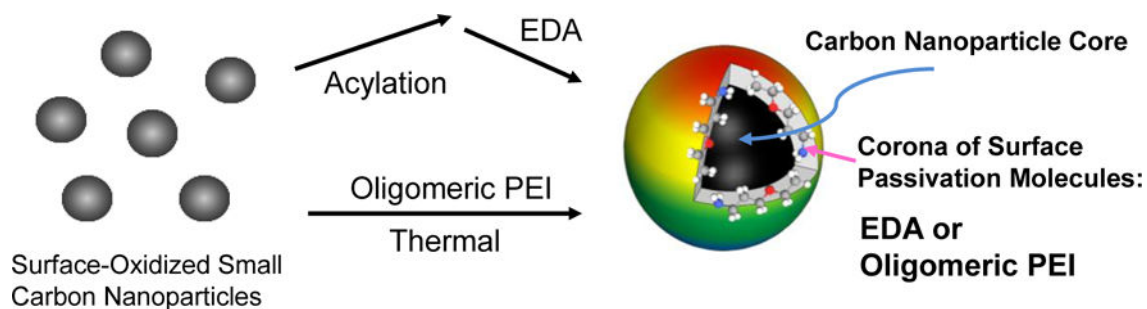


Figure 1.

A cartoon illustration on reaction schemes based on chemical functionalization (amidation with 2,2'-(ethylenedioxy)bis(ethylamine) or EDA,²⁹ as an example) and on the thermally induced functionalization with oligomeric polyethyleneimine (PEI). For the cartoon on carbon dot, it is generally a small carbon nanoparticle core with attached and strongly adsorbed surface passivation molecules (a configuration similar to a soft corona).

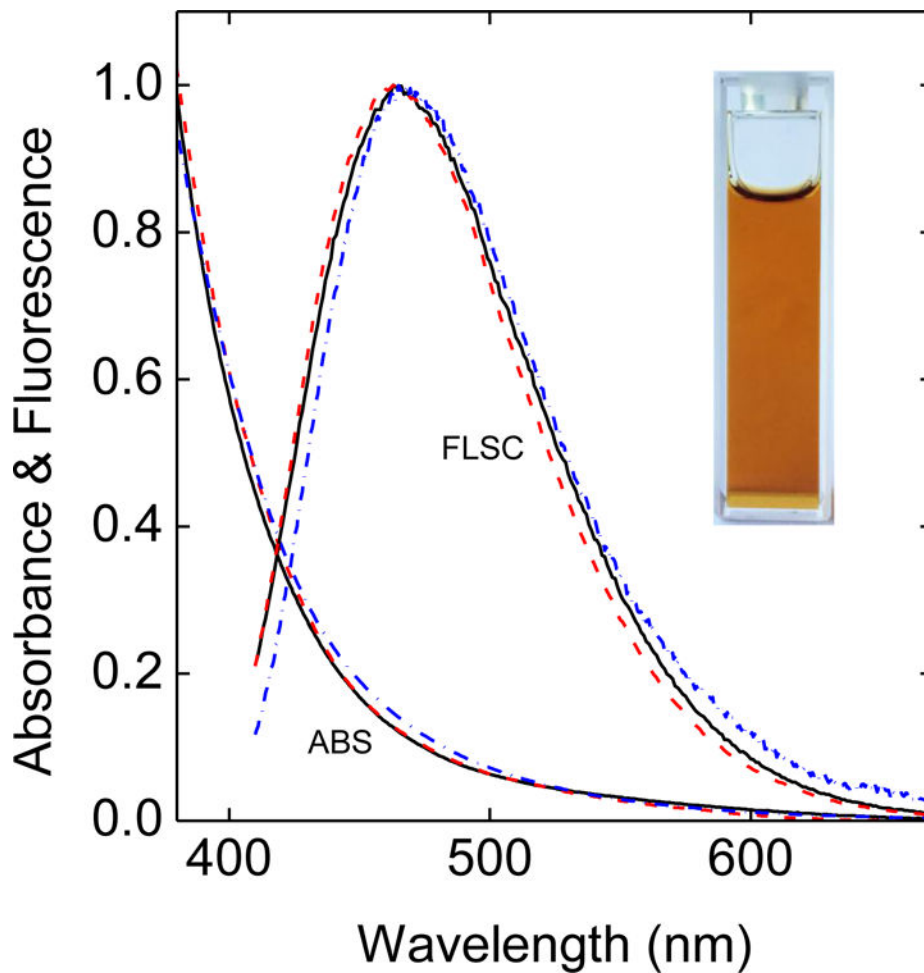


Figure 2. Absorption (ABS) and fluorescence (FLSC, 400 nm excitation) spectra of PEI-carbon dots in aqueous solutions (solid line: as-synthesized; dash line: the more fluorescent sample from fractionation), and the spectra of the EDA-carbon dots (dash-dot line)²⁹ also shown for comparison. Inset: A photo on an aqueous solution of the PEI-carbon dots.

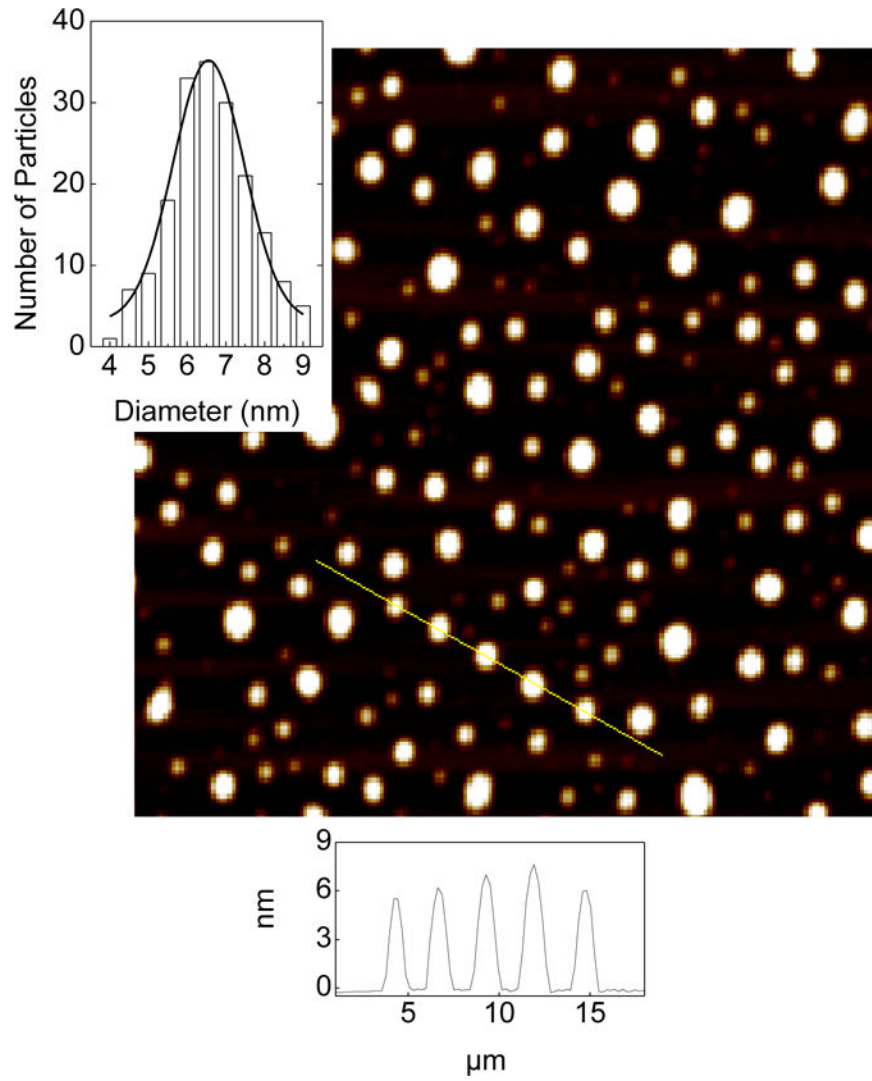


Figure 3. An AFM image on the PEI-carbon dots on mica surface, with height analyses of the selected dots. Inset: A statistical analysis of the size data from height analyses of more than 150 dots in multiple AFM images.

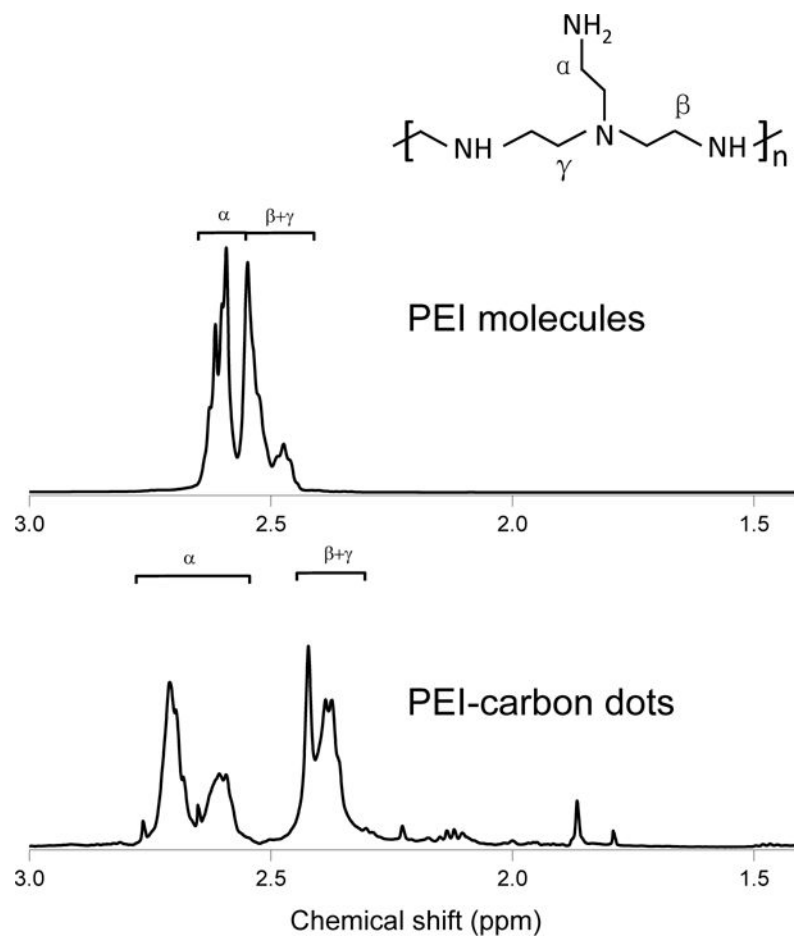


Figure 4. The proton NMR spectra of neat PEI (top, with the different groups of protons marked in the chemical structure) and the PEI-carbon dots (bottom) in deuterated water.

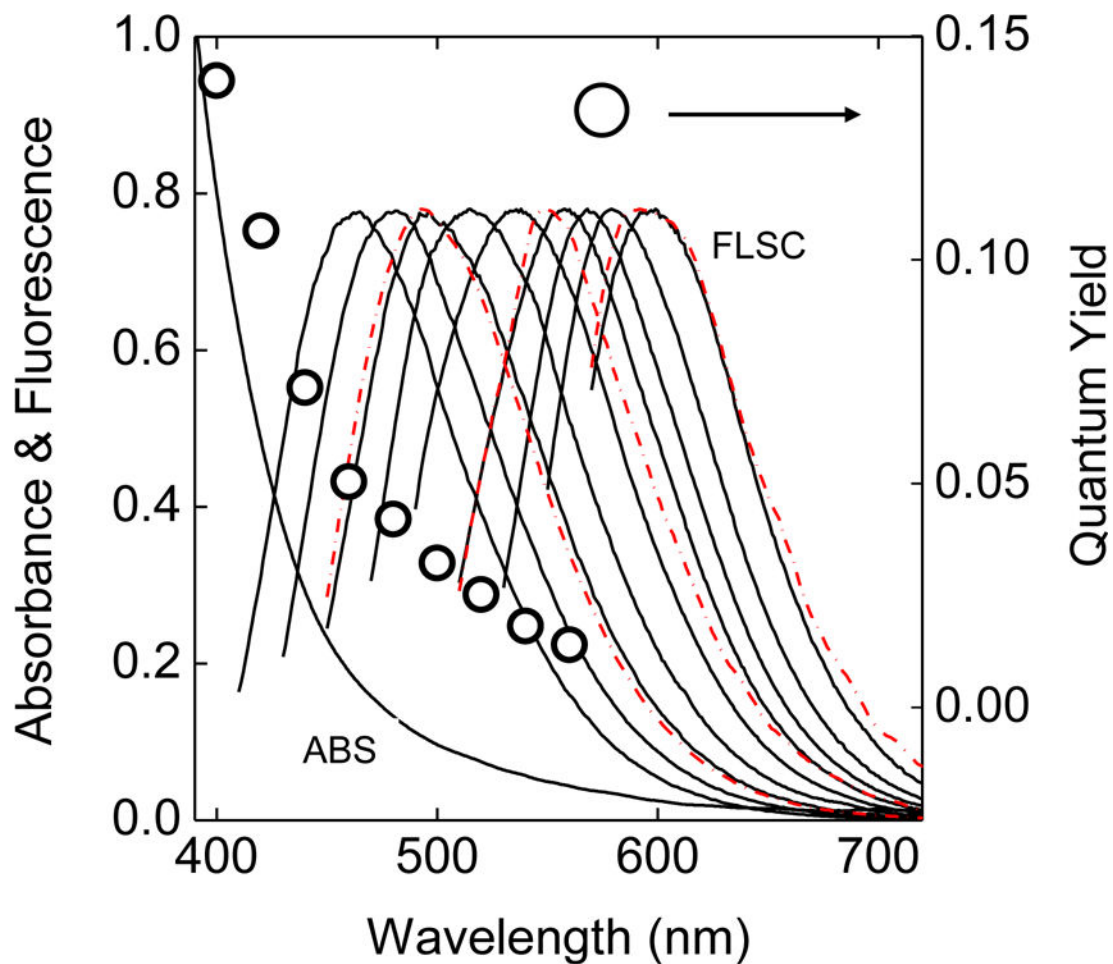


Figure 5. Absorption (ABS) and fluorescence (FLSC) spectra and quantum yields of the PEI-carbon dots at different excitation wavelengths (spectra in solid lines from left to right corresponding to excitation wavelengths from 400 nm to 560 nm in 20 nm increment). The spectra of the EDA-carbon dots (dashed lines)²⁹ at 440 nm, 500 nm, and 560 nm excitations are also shown for comparison.

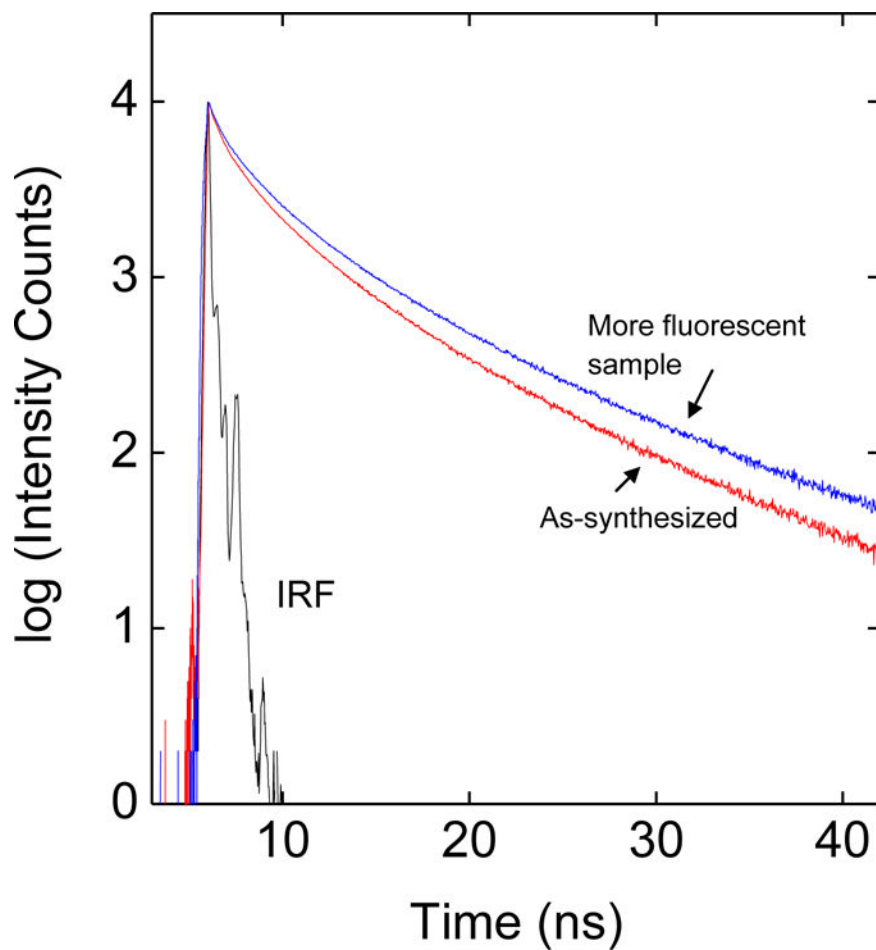


Figure 6. Observed fluorescence decays of the as-synthesized PEI-carbon dots and the more fluorescent sample from fractionation (400 nm excitation).

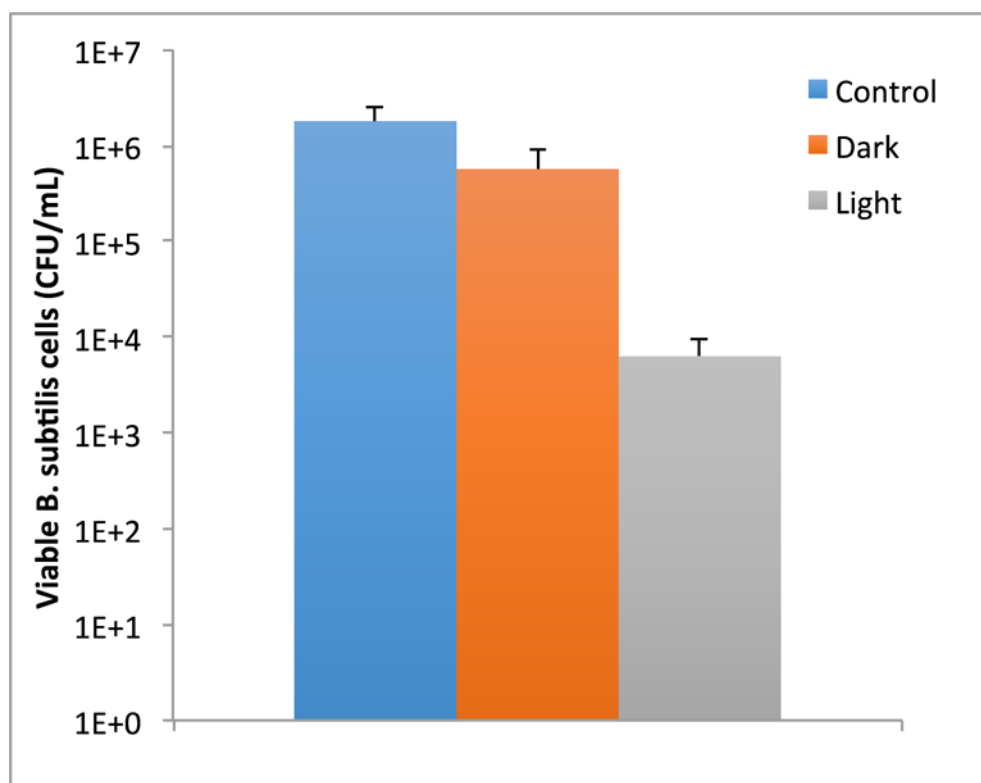


Figure 7. Results on the viable cell number reduction after *B. subtilis* cells were treated with the PEI-carbon dots (0.02 mg/mL) in the dark and with 1 h visible light illumination. Data are shown as mean \pm standard deviation from triplicate tests.

Results from the Deconvolution of Observed Fluorescence Decays with a Bi-Exponential Function

Table 1

Sample	λ_{EX} (nm)	λ_{EM} (nm)	τ_{F1} (ns)	A_1 (%)	τ_{F2} (ns)	A_2 (%)	$\langle\tau_F\rangle^a$ (ns)	Φ_F
As-synthesized	400	480	0.7	9	3.3	91	3.2	0.12
	440	520	0.6	7	2.9	93	2.9	0.07
More fluorescent sample from the fractionation	400	480	0.9	8	4.4	92	4.3	0.22
	440	520	0.7	8	3.7	92	3.7	0.12

^aThe average fluorescence lifetime $\langle\tau_F\rangle = (A_1 \tau_{F1}^2 + A_2 \tau_{F2}^2) / (A_1 \tau_{F1} + A_2 \tau_{F2})$ (see ref. 38).